Turkish Journal of Civil Engineering, 2025, 59-91, Paper 805, ***Research Article***

A Review of Punching Shear Strength in FRP-Reinforced Concrete Slab-Column Connections

Ragheb SALIM[1*]

ABSTRACT

This review explores the use of Fiber Reinforced Polymer (FRP) bars to reinforce concrete slab-column connections, highlighting their potential to extend service life, reduce maintenance costs, and improve life-cycle cost efficiency. FRP bars offer a more environmentally friendly alternative to traditional steel reinforcement. The shear behavior of reinforced concrete structural members, which depends on complex internal load-carrying mechanisms, remains an active area of research. This article provides a comprehensive overview of the punching shear strength and behavior of FRP-reinforced concrete (FRP-RC) slab-column connections, both with and without FRP stirrups for shear reinforcement. It examines the mechanisms of punching shear in FRP-RC slab-column connections and reviews existing codes, proposed or modified models, and machine learning approaches for predicting the punching shear strength of these connections.

Keywords: Slab-column connection, punching shear capacity, FRP bar, machine learning, design model.

1. INTRODUCTION

The corrosion of steel reinforcement stands out as a primary durability issue in reinforced concrete (RC) structures, posing a significant threat to their longevity and incurring substantial maintenance costs. In severe instances, corrosion can precipitate unforeseen and severe failures in RC structures. This deterioration is compounded by the degradation of the bond between concrete and steel reinforcement as corrosion progresses, further weakening the structure [1-2]. Moreover, corrosion might result in a reduction in the steel reinforcement's cross-sectional area, which lowers its tensile strength and ductility [3-4]. As a result, several strategies to reduce the danger of corrosion have been proposed and developed. These include of using low-permeable or impermeable concrete, adding thickness to the concrete cover, utilizing coated or stainless steel bars, and putting waterproofing

Note:
- This paper was received on June 7, 2024 and accepted for publication by the Editorial Board on January 15, 2025.
- Discussions on this paper will be accepted by July 31, 2025.
- https://doi.org/10.18400/tjce.1497261

1 Çukurova University, Department of Civil Engineering, Adana, Türkiye
r.salim@gu.edu.ps - https://orcid.org/0000-0003-2283-501X
* Corresponding author

measures in place [5-7]. One possible solution to corrosion problems in concrete structures is the adoption of modern composite materials, like fiber-reinforced polymer (FRP) bars, which have gained increased popularity in recent times. Utilizing FRP bars offers multiple advantages; besides their exceptional resistance to corrosion in harsh environmental conditions (such as salt exposure for deicing, freeze-thaw cycles, and wet-dry cycles), they boast a high strength-to-weight ratio and are non-magnetic [8]. The use of FRP bars as flexural and shear reinforcement in concrete structures has been the subject of several experimental studies with the goal of improving knowledge of their effects on the structural performance of FRP-reinforced concrete (FRP-RC) elements such as beams, slabs, and columns [9-11]. Because punching shear failure in concrete slab-column connections is usually abrupt and brittle, and frequently happens suddenly, a great deal of attention has been focused on researching it. Such failures might cause partial floor damage or possibly collapse structurally [12-13]. According to Matthys and Taerwe [14], assuming equivalent flexural stiffness, concrete slabs reinforced using carbon fiber reinforced polymer (CFRP) grids for flexural reinforcement showed a punching shear capacity similar to that of conventional concrete slabs reinforced with steel. According to research by Ospina et al. [15], the flexural stiffness of the FRP reinforcement and the strength of the bond between the concrete and the FRP are the two main elements determining the punched shear strength of FRP-RC slab-column connections. Furthermore, it was noted that the punching shear capabilities of concrete connections reinforced with FRP bars and grids varied. These variations were ascribed to variations in bonding characteristics and stress distribution at the FRP grid intersections. Lee et al. [16,17] demonstrated that boosting the glass fiber reinforced polymer (GFRP) reinforcement ratio within 1.5 times the slab thickness (denoted as 'h') from the column face enhances the punching shear strength of concrete slabs. Nevertheless, it was discovered that adding more GFRP reinforcement than 3% will not increase the GFRP-RC slabs' punching shear capability [16]. Dulude et al. [18] observed a notable increase in the punching shear strength of FRP-RC slabs with larger slab thicknesses and column sizes. Likewise, employing higher strength concrete yielded a similar enhancement [19].

Concrete slab-column connections' punching shear strength may be greatly increased by adding steel shear reinforcement, as is well known [20, 21]. Previous studies reporting the use of FRP bars as shear reinforcement have shown similar findings [22–26]. A range of shear reinforcing methods, such as CFRP shear bands [22], CFRP rods [23], CFRP shear rails [24], GFRP and CFRP spiral stirrups [25], and double-head GFRP bars used as shear studs [26], have been presented by research investigations to improve the punching shear strength of FRP-RC slabs. By minimizing bond-slip and postponing the propagation of cracks around column faces, these reinforcing techniques successfully avoid punching shear failure at lower load values [27]. Punching shear strength can be further increased by using FRP stirrups that are properly secured [28].

To calculate the punching shear strength of connections between FRP-RC slabs and columns, a number of design equations have been put forth. These formulae were obtained in two ways: either by modifying the design formulas already in use for traditional RC slabs reinforced with steel [14, 29–31], or by conducting restricted tests [15]. Several analytical models have been introduced, such as Theodorakopoulos and Swamy's [32] model, which is based on moment-shear interaction. This model aims to forecast the punching shear strength of FRP-RC slab-column connections. The depth of the compression zone, which is influenced by the FRP reinforcement's tensile strength and elastic modulus as well as the

bonding properties between the concrete and the reinforcement, is the main emphasis of the model. A semi-empirical fracture mechanics-based model was devised by Nguyen-Minh and Rovnak [33] to assess the punching shear resistance of internal GFRP-RC slab-column connections. This model takes into account many aspects, including the anchorage effect of flexural reinforcement, the span-to-depth ratio (L/d), and the size impact. Moreover, a number of other design formulae for FRP-RC slabs with FRP shear reinforcement are available in the literature. To allow for FRP shear reinforcement, Gouda and El-Salakawy [26] and Salama et al. [31] suggested changes to the CSA/S806-12 [34] code. According to Gouda and El-Salakawy [26], concrete contributes 75% of what FRP-reinforced concrete components lacking shear reinforcement do within the shear-reinforced zone. On the other hand, Salama et al. [31] recommended, contrary to CSA/S806-12 [34], that the shear strength be calculated taking into account the shear reinforcement with a maximum strain limit of 0.005, as well as half the shear strength given by concrete inside the shear-reinforced zone. Similarly, Hassan et al. [35] proposed that, compared to concrete lacking shear reinforcement, the shear strength contributed by concrete in the area reinforced for shear should be halved. Furthermore, they recommended using the allowable stress for FRP shear reinforcement to determine the shear strength provided by the shear reinforcement.

Despite the wealth of research on resistance to punching shear in FRP-reinforced concrete slab-column connection, there remains a notable gap in the literature: a comprehensive synthesis of findings consolidated into a single resource. This study endeavors to fill this gap by undertaking a thorough examination of various aspects, including FRP properties, the mechanics behind punching shear failure, and the efficacy of FRP shear reinforcement in enhancing punching shear strength. In particular, it looks into two main situations: the punching shear resistance of FRP-RC slab-column connection lacking FRP shear reinforcement, and those incorporating such reinforcement. Additionally, the study scrutinizes mathematical and numerical models aimed at predicting punching shear strength. Drawing from a meticulous review of approximately one hundred research papers, this analysis aims to provide a consolidated understanding of punching shear strength in FRP-reinforced concrete slab-column connections.

2. FRP COMPOSITE MATERIALS

In 1975, the earliest application of fiber reinforced polymer (FRP) was seen in Russia, specifically in the form of reinforcement bars [36,37]. Fiber reinforced plastic, or FRP, is a category of materials that use natural or synthetic fibers to naturally increase the strength and stiffness of a polymer matrix [37]. FRPs utilized for strengthening and reinforcing structures boast immense strength, being rated as eight times stronger than traditional steel reinforcement bars [38]. Glass fiber reinforced polymer (GFRP) is employed as prestressing tendons to enhance the strength of a 9-meter-long wooden bridge that is securely fastened [39]. In Europe, research on the potential of fiber-reinforced polymers (FRPs) as a substitute for steel plate bonding in bridge repair and reinforcement began in the 1980s. On the other hand, FRP composites have been used for structural strengthening in the US for around 25 years [40]. Throughout this timeframe, the acceptance of FRP composite as a prevalent construction material rose in tandem with the increasing number of successful FRP strengthening projects. Among design consultants, the adoption of FRP for strengthening, rehabilitation, and retrofitting gained significant traction, surpassing traditional methods like

installing additional structural steel frames and components [41]. FRP is primarily utilized as internal reinforcement, such as rebar, or externally bonded reinforcement to enhance the strength of concrete, timber, steel, and masonry structures [42]. During the 1990s in Japan, FRP bars garnered considerable attention due to their involvement in the study of notably elevated train support structures [43]. Not only does FRP weigh only 25% of steel, but it also has a unique tensile strength attribute that exceeds steel's [36–43]. The Japanese group was the first to publish design recommendations for using fiber reinforced polymer (FRP) to strengthen reinforced concrete (RC) buildings in 1996 [43, 44]. Since then, the use of FRP as a structural reinforcement has grown exponentially, leading official organizations all over the world to create design supervision and guidance guidelines [45, 46]. Design regulations for seismic upgrades of structures have long supported the use of externally bonded fiber reinforced polymer (FRP) reinforcement for reinforcing structural elements, particularly when using high-strength CFRP. Notably, there has been a recent surge in interest towards developing economical and efficient methods for repairing, upgrading, strengthening, or reinforcing existing RC bridges [47, 48]. Rebuilding an existing RC bridge is usually driven by two primary concerns: the need to address deterioration that has accumulated over years of use and the need to increase the bridge's strength to keep up with increases in the weight of contemporary vehicles [49–55]. FRP reinforcements can be used to increase an element's structural load-bearing capability [38,56,57].

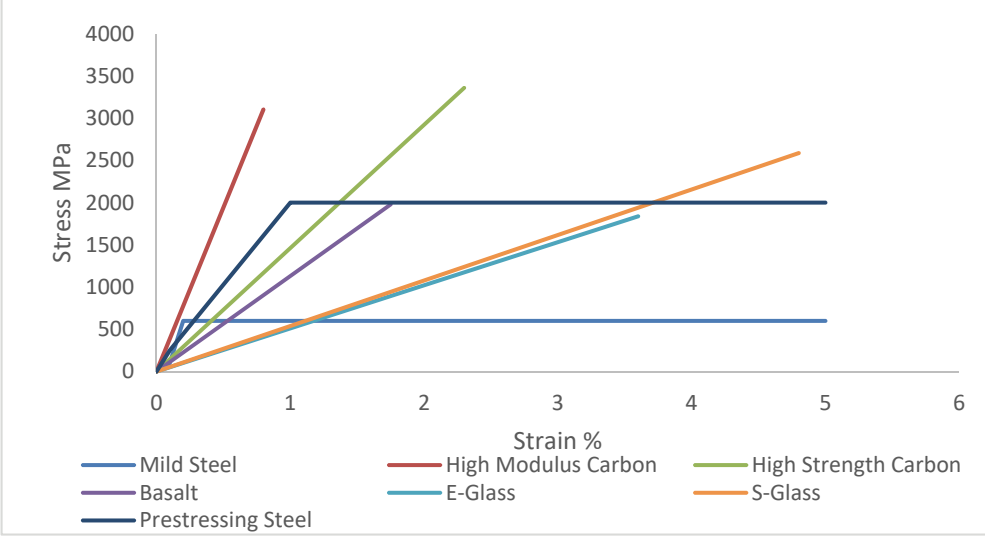

Figure 1 - Comparative analysis between FRP materials and steel [39]

The most widely used FRP composite reinforcements in civil engineering are made by pultruding carbon fiber (CFRP), glass fiber (GFRP), basalt fiber (BFRP), and aramid fiber (AFRP) [58,59]. Among structural FRPs, E-GFRP stands out as the most economical material and consequently enjoys the highest consumption rate [60]. In contrast to E-GFRP, BFRP carries a higher cost due to limited manufacturing capacity. Nevertheless, its price is justified by its superior strength compared to GFRP, along with its resistance to alkalis and

its nearly inexhaustible resource base [38]. With an emphasis on their stress-strain characteristics, Figure 1 presents a thorough comparison of FRP materials and steel reinforcements. Because of its high cost and limited compressive strength independent of the direction of fiber alignment, AFRP is not commonly used as a structural bar, despite its promise [61, 62]. Aramid fiber stands out as the optimal choice for ballistic-resistant fabrics, as it effectively absorbs impact energy [63]. CFRP exhibits the highest strength among FRP materials and boasts the widest range of strengths available [64]. This diversity arises from differences in carbon sources and manufacturing methods. Comparing CFRP to other FRP materials, however, CFRP shows a higher resilience to fatigue and creep failure [65]. Due of its remarkable strength and resistance to fatigue and cycle failures, CFRP is more expensive than other materials [66–68].

Materials of FRP bars are often classified and identified based on their mechanical properties. Table 1 provides an overview of the mechanical properties of the most commonly available FRP bars on the market.

Table 1 - Overview of mechanical properties for various types of FRP materials [41]

Material type	**Density** (kg/m^3)	Tensile strength (MPa)	**Young's** modulus (GPa)	**Elongation (%)**
CFRP	1500-2100	600-3920	37-784	0.5-1.8
GFRP	1250-2500	483-4580	35-86	1.2-5.0
AFRP	1250-1450	1720-3620	41-175	1.4-4.4
BFRP	1900-2100	600-1500	50-65	1.2-2.6
Steel	7850	483-690	200	6.0-12.0

Fiber-reinforced polymer (FRP) composite materials exhibit notable durability [69–71] and offer a reasonable fatigue life [72,73]. Their high strength-to-weight ratios make them adaptable to various shapes and sizes of structures with ease. Additionally, FRPs demonstrate corrosion resistance and robust weather resilience. They excel in chemical resistance across a spectrum of substances. Furthermore, their lightweight nature significantly reduces labor costs. As the composite industry continues to advance, focusing on high-performance materials for aging civil engineering infrastructure, FRP stands poised to significantly extend the service life of global infrastructure throughout this century.

3. PUNCHING BEHAVIOR OF STEEL-REINFORCED CONCRETE (RC) SLABS

Punching shear failure in reinforced concrete flat slabs happens locally around the support regions due to intense shear and bending stresses. This type of failure is characterized by the development of a truncated cone shape, which results in a rapid and substantial decrease in the slabs' load-bearing capacity [74]. The evolution of the process leading to punching failure unfolds through several stages as illustrated in Figure 2 [75]: Initially, an approximately circular crack initiates around the column edge on the tension surface of the slab, penetrating deeply in the direction of the compression area. Afterward, a fresh lateral and flexural crack

appears. Next, an inclined shear crack develops near the midpoint of the slab depth, often occurring when the load approaches approximately half to two-thirds of its load-carrying capacity. As the loading persists, these diagonal cracks extend across both the areas experiencing tension and compression, typically at angles varying between 25 and 45 degrees. Ultimately, the diagonal cracks advance to the juncture where the slab meets the support, indicating the failure point at the punching load. The ability of slabs to withstand punching shear is commonly affected by particular factors concerning geometry and material characteristics. These factors include the size of the support cross-section, depth of the slab, strength of the concrete, and the proportion of longitudinal reinforcement [76].

Figure 2 - Punching shear failure mechanism observed in reinforced concrete flat slabs [75]

In the absence of shear reinforcement, inclined cracks trigger the resistance of shear stresses through five key elements of concrete shear strength, as identified by the ASCE-ACI Committee 426 [77]. These factors include: (1) Vc denotes the shear resistance within the compression zone, where the concrete remains uncracked.; (2) Va pertains to the interlocking of aggregates along the surfaces of cracks; (3) Vd relates to the dowel action enabled by flexural reinforcement intersecting the shear crack; (4) Arch action, especially noticeable in deep members with a shear span-to-depth ratio less than 2.5; and (5) Residual tensile stresses within the shear crack arise from minor connections between its surfaces. The ultimate shear strength of slabs generally exceeds that of beams, a phenomenon explained by the ASCE-ACI Committee 426 [77]. This discrepancy can be attributed to several influential factors. Firstly, the allocation of bending moments within a slab differs from that in beams. Secondly, slabs lack the balancing effect present in beams. Thirdly, conventional static analysis may prove inadequate in fully capturing slab behavior. Additionally, in-plane forces exerted by supports' restraints contribute to the overall strength of slabs. Finally, the interplay between bending and shear effects further enhances the shear resistance of slabs.

Two different kinds of bending moments-radial and tangential moments-have an impact on the slab at the contact between it and the column. The first fracture usually appears as a tangential flexural crack close to the column face, where the radial moment is highest, when the material is initially exposed to vertical shear force. Following this, the tangential moment causes radial fractures to emerge from the column faces. Further tangential cracks that are located further from the column face only become visible when there is a significant increase in applied load because the radial moment rapidly decreases in the direction of the column face. On the other hand, the beginning of inclined fractures proceeds in a different way since they spread perpendicular to radial cracks. Because inclined fractures may only occur in places where flexural tangential cracks are not present, these cracks often start in the middle

of the slabs. As a result, instead of having the same characteristics as flexural-shear fractures seen in beams, they have web-shear crack features. In this case, a mechanism absent in beams governs the beginning of inclined cracks: the rigidity of the slab in the lateral direction [78].

Lenschow and Sozen [79] observed that slabs commonly employ orthogonal reinforcement mats, resulting in an intricate distribution of in-plane forces throughout the structure. A slab section with a reinforcing mat positioned at a 45-degree angle to the direction of the moment, M1, is shown in Figure 3. When there is no moment in the y direction (M2 = 0), The separate elements of the reinforcement forces, denoted as T, in the y-axis direction are counteracted by compressive forces within the concrete at the reinforcement level. As a result, if flexural fractures diverge from parallel alignment with the reinforcement, in-plane forces appear within the section of the slab where reinforcement is present. These in-plane forces increase the applied loads, which contribute to the advancement of further cracking after the first fractures.

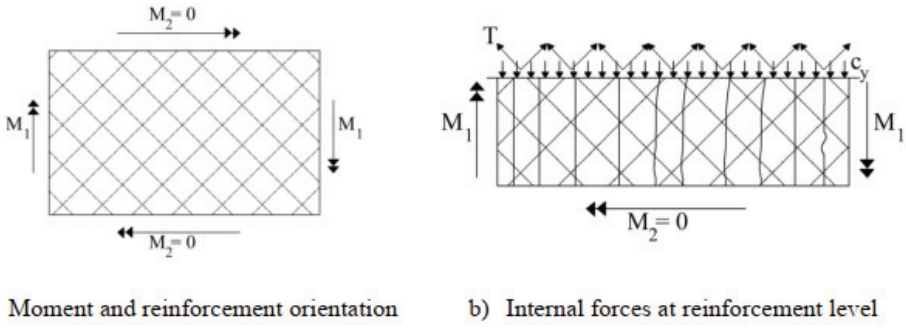

Figure 3 - The lateral forces within slabs, as described by ASCE-ACI Committee 426 [77]

Figure 4 shows the balance of internal forces along diagonal cracks within both slab and beam structures. Concerning the beam (depicted in Figure 4a), sustaining equilibrium requires the tensile force, T, in the reinforcement spanning the diagonal crack to counterbalance the compressive force, C, applied above the fracture. Conversely, in the case of the slab (Figure 4b), equilibrium doesn't demand that the compressive force, C1, beneath the inclined crack, equals the tensile force, T1, generated in the reinforcement spanning the fracture. To sustain equilibrium, it is essential for the total compressive forces across the entire width of the slab, expressed as C1+C2, to be equal the cumulative tensile forces within the reinforcement across the width of the slab, indicated as T1+T2. While fulfilling equilibrium criteria, the transfer capability of force C1 and the proportion of C1 to C2 might diminish with the reduction in uncracked concrete depth at the inclined crack location. However, there is no corresponding mechanism for decreasing shear forces at this point. Although reinforcing around the failure perimeter seems to enhance compressive force C1 by increasing the depth of uncracked concrete, the tensile force T1 within the reinforcement can be counteracted by compressive force C2 beyond the failure perimeter [77–79].

In the cracked area near the column, outward in-plane displacements are frequently observed in slabs. However, the stiffness of the surrounding slab resists these displacements, resulting in in-plane compression forces within the slab. As a result, these pressures increase both the

bending and the shear capacities of connections between slabs and columns. Conversely, they restrict the rotations of cross-sections, thus increasing susceptibility to brittle punching failure [77].

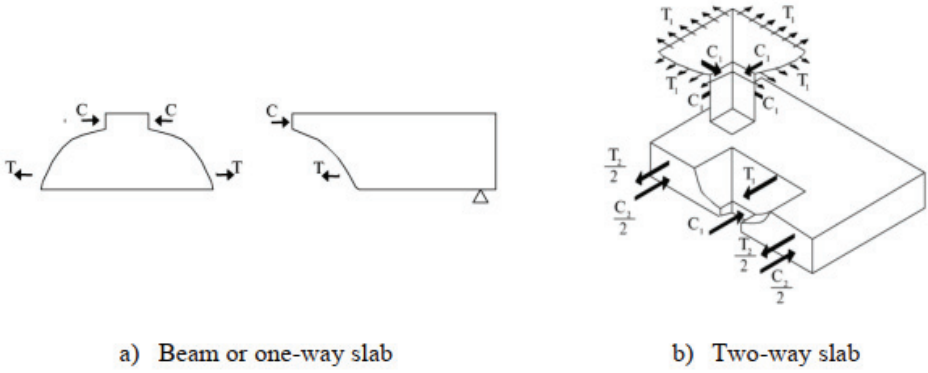

Figure 4 - Forces observed at inclined cracks, as documented by ASCE-ACI Committee 426 [77]

In slab-column connections, the regions crucial for both moment and shear are typically concentrated near the column. This convergence leads to an anticipation of moment-shear interaction, complicating the distinct classification of failures as purely flexural or punching failures in numerous instances. Typically, when the slab's reinforcement ratio increases, the failure modes shift from flexural to punching failure. [77, 78].

4. PUNCHING SHEAR STRENGTH OF FRP-RC SLAB-COLUMN CONNECTIONS WITHOUT SHEAR REINFORCEMENT

Concrete flexural cracking and steel reinforcement yielding are typical prior to punched shear failure in structural members subjected largely to flexural pressures, like reinforced concrete slab-column connections [80]. The punching shear resistance of steel-reinforced concrete (RC) slabs primarily relies on the intact concrete within the compression zone, dictated by the tensile reinforcement's resultant force [81,82]. Similar failure modes have been observed in FRP-RC slabs [16,17,19]. However, due to the superior strength of Fiber-Reinforced Polymer reinforcement as opposed to steel reinforcement and its retention of linear elastic behavior until failure, punching shear failure in slabs reinforced with FRP typically happens later than in steel-RC slabs with the same reinforcement area. In FRP-RC slabs, punching shear failure often transpires before the FRP reinforcement ruptures [18].

Banthia et al. [83] undertook a comprehensive investigation into the efficacy of FRP grid reinforcement in concrete slabs, juxtaposing its performance against that of steel-reinforced counterparts. Plots of load against load point displacement were created by careful testing under transverse loads in order to understand the behavior of the slabs. The application of fiber-reinforced concrete and variances in concrete strength were closely examined in this study, and strain measurements were methodically recorded at various grid positions. The

findings unveiled that FRP-reinforced slabs exhibited either comparable or superior ultimate loads compared to steel-reinforced slabs. However, a notable drawback surfaced: the inherent brittle fracture nature of FRP led to diminished energy absorption capacities relative to their steel counterparts. In a complementary endeavor, Matthys and Taerwe [14] investigated the punching capacity of slabs reinforced with various FRP grid configurations, directly contrasting them with steel-reinforced counterparts. Intriguingly, for FRP-reinforced slabs boasting equivalent flexural strength to their steel-reinforced counterparts, the punching load and stiffness in the cracked state experienced significant reductions. This observation underscores the pivotal role of grid bond behavior in shaping crack propagation dynamics and, ultimately, the brittleness of punching failure. El-Ghandour et al. [22] present the outcomes of a detailed two-phase experimental program aimed at investigating the punching shear behavior of fiber reinforced polymer-reinforced concrete (FRP-RC) flat slabs, both with and without carbon fiber reinforced polymer (CFRP) shear reinforcement. In the initial phase, the study identified issues related to bond slip and crack localization. Subsequent adjustments made in the second phase, particularly the reduction in spacing between flexural bars, effectively addressed these concerns, leading to the occurrence of punching shear failure in the slabs. However, despite these modifications, CFRP shear reinforcement was found to be inefficient in significantly enhancing the slab capacity due to its inherent brittleness. In a related study, Li et al. [84] investigated the behavior of flat plate slabs reinforced with CFRP rods in the punching shear zone. These slabs were subjected to constant gravity load and lateral displacements in a reversed cyclic manner. The research involved testing three specimens of interior column-slab connections: one standard specimen without shear reinforcement, a second reinforced with CFRP rods, and a third reinforced with stud rails, serving as a reference to the second specimen. While punching shear failure occurred in the standard specimens at a lateral drift ratio of approximately 5%, the specimen reinforced with CFRP rods displayed significant flexural yielding. It sustained deformations up to a drift ratio of approximately 9% without notable strength losses and did not experience punching shear failure. Additionally, displacements in this specimen were up to 1.79 times larger than those of the standard specimen, indicating a 42% superior ductile performance compared to the standard specimen, and even matching the capability of the stud rail reinforced specimen. These experimental findings suggest a promising outlook for the utilization of CFRP rods in flat slab applications.

Lee et al. [16] delved into the comparison between glass fiber-reinforced polymer (GFRP) and steel bars in terms of their impact on punching shear resistance. Their experimental findings delineated clear disparities: Due to the lower elastic modulus of GFRP bars, slabs reinforced with GFRP exhibited notably reduced punching shear capacities, decreased post-cracking stiffness, and increased deflections compared to their steel-reinforced counterparts. Additionally, GFRP-reinforced slabs showed a heightened propensity for crack formation in the immediate column region relative to those reinforced with steel bars. In a similar vein, Hussein and Rashid [85] meticulously investigated the punching-shear behavior of two-way concrete slabs reinforced with varying grades of GFRP bars. Employing monotonic concentric loading until failure, the experimental setup allowed for a comprehensive evaluation of reinforcement type and ratio effects. Notably, the tested specimens exclusively experienced punching-shear failure as the final mode, with no instances of concrete flexural crushing, rupture, or slippage failure of the reinforcing bars observed. Moreover, their study

revealed that an increase in GFRP reinforcement ratio led to enhanced punching-shear capacities, reduced strains in the reinforcement, and minimized slab deflections.

In a thorough investigation, Shill et al. [86] compared the structural behavior of extensive two-way concrete slabs reinforced with fiber-reinforced polymer (FRP) rebars to that of traditional steel-reinforced concrete. In place of steel reinforcement, basalt fiber composites (BFRP) and carbon fiber composites (CFRP) were also assessed. Comparing CFRP-RC and BFRP-RC slabs to steel-RC slabs, the testing results showed that the former had cracking moment capabilities that were around 7% and 4% greater, respectively. It is worth mentioning that the two types of FRP-RC exhibited different load capacity behaviors: CFRP-RC slabs displayed a rapid decrease in load capacity similar to steel-RC slabs, while BFRP-RC slabs demonstrated a gradual reduction beyond the peak load. Additionally, BFRP-RC slabs exhibited 1.72 times more ductility compared to CFRP-RC slabs. The collapse of FRP-RC slabs resulted from punching shear, whereas the failure of the steel-RC slab was due to flexural bending moment. Steel rebars were found to have yielded upon failure, whereas FRP rebars remained intact. Moreover, FRP-RC slabs exhibited more fractures and deflection compared to steel-RC slabs. However, FRP-RC slabs demonstrated elastic recovery after unloading, a behavior not observed in steel-RC slabs.

4.1. Punching Shear Strength of FRP-RC Slab-Column Connectors without Shear Reinforcement: Analytical Models

4.1.1. Codes Specified Formulas

The critical shear perimeter method forms the basis of various design codes, such as ACI 318-19 [87], CSA-A23.3-04 [88], BS 8110-97 [89], and CEB-FIP 90 [90]. This methodology is derived exclusively from extensive test data [91,92]. Instead of relying solely on empirical

Table 2: Critical shear perimeters as defined by various codes and standards.

Model based on perimeter	ACI 318-19 [87], CSA-A23.3-04[88] and JSCE [94]	BS 8110-97 [89]	CEB-FIP 90 [90]
Key perimeter	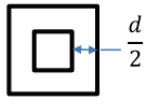 $b_c = 4(c + d)$	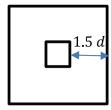 $b_c = 4(c + 3d)$	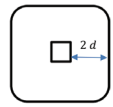 $b_c = 4(c + \pi d)$
	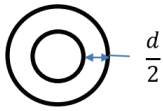 $b_c = \pi(c + d)$	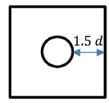 $b_c = 4(c + 3d)$	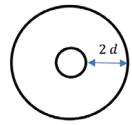 $b_c = \pi(c + d)$

models, Model Code 2010 [21] integrates punching shear equations rooted in the mechanical concept of critical shear crack theory (CSCT) introduced by Muttoni [93]. These equations utilize the maximum shear stresses along an imaginary vertical critical perimeter surrounding the column to determine punching shear strength. Punching shear capacity in the CSCT model is dependent on the size and texture of shear fractures created by slanted compression struts that withstand shear loads. These design guidelines and standards offer distinct formulations for punching shear calculations, with significant differences in the crucial perimeter's form and placement. Various critical shear perimeters are offered, based on statistical studies and the characteristics taken into account by each design code. An overview of the essential shear perimeter anticipated for each design code is shown in Table 2. The models provided by several researchers as well as those defined by rules and standards are covered in detail in the following sections.

The ACI 318 code equation was modified with the addition of a modification factor k in ACI 440.1R-15 [95]. By incorporating this adjustment, the aim was to ensure that the punching shear strength of FRP-reinforced two-way concrete flat slabs reflects the impact of both the reinforcement ratio and the variable elastic modulus of FRP bars. The following is the equation given in ACI 440.1R-15 [95]:

$$V_R = 0.8\sqrt{f_c'}\, b_{\circ ACI} dk \tag{1}$$

$$k = \sqrt{2\rho n_t + (\rho n_t)^2} - \rho n_t \tag{2}$$

Here, n_t represents the modular ratio, defined as the ratio of the modulus of elasticity of FRP (Ef) to that of steel (Es). Meanwhile, ρ denotes the reinforcement ratio.

CSA S806-12 [96] introduced significant modifications to the punching shear equation originally designed for steel-reinforced concrete flat slabs in CSA-A23.3-04 [88], tailoring it for application in FRP-reinforced flat slabs. This revised formula takes into consideration a number of factors, including size effect, reinforcement stiffness, reinforcement ratio, and concrete compressive strength, that influencing the punching shear resistance of two-way flat slabs. The minimal value derived from the given equations is used to calculate the punching shear capacity of FRP-reinforced concrete flat slabs, per CSA S806-12 [96]:

$$V_R = \left(1 + \frac{2}{\beta}\right) 0.028\lambda\left(E_f\, \rho_f f_c'\right)^{1/3} b_{\circ CSA} d \tag{3}$$

$$V_R = \left(\frac{a_s d}{b_{\circ CSA}} + 0.19\right) 0.147\lambda\left(E_f\, \rho_f f_c'\right)^{1/3} b_{\circ CSA} d \tag{4}$$

$$V_R = 0.056\lambda\left(E_f\, \rho_f f_c'\right)^{1/3} b_{\circ CSA} d \tag{5}$$

Here, ρ_f represents the reinforcement ratio of FRP.

In JSCE 1997 [94], an equation for designing punching shear in FRP-reinforced concrete slabs was presented. This equation encompasses all primary parameters affecting punching shear strength and is structured as follows:

$$V_R = \beta_d \beta_p \beta_r f_{pcd}\, b_{\circ JSCE} d \quad (6)$$

where:

$$\beta_d = \left(\frac{1000}{d}\right)^{1/4}$$

$$\beta_p = \left(\frac{100\rho_f E_f}{E_s}\right)^{1/3}$$

$$\beta_r = 1 + 1/\left(1 + \frac{0.25u}{d}\right)$$

$$f_{pcd} = 0.8\sqrt{f_c'} \leq 1.2 \text{ MPa}$$

where $b_{\circ JSCE}$ the critical shear perimeter specified by JSCE [94] closely resembles that outlined in ACI 318–19 [87]. Here, u denotes the perimeter of the column.

4.1.2. Proposed or Modified Models

A comparative examination of the observed values for FRP-reinforced slabs lacking shear reinforcement available in the literature and the punched shear strength estimations obtained using the suggested formula is shown in Table 3. Rizk et al. [97] proposed a modification to the formula in ACI 318-11 for calculating the punching shear capacity of steel-reinforced concrete slabs, which can be extended to FRP-reinforced slabs by incorporating adjustments for the material properties of FRP, such as its lower stiffness and distinct tensile behavior:

$$V_R = 0.333\sqrt{f_c'}\left(\frac{l_{ch}}{h}\right)^{0.333}(100\rho)^{0.333} b_{\circ ACI} d \quad (7)$$

Here, l_{ch} denotes the characteristic length, defined as $-0.84f_c'$+500 based on the approach outlined by Zhuo et al. [98], while h represents the thickness of the slab.

Conversely, Rizk et al. [99] employed regression analysis to adjust the CSA-A23.3–04 equation used for predicting the punching shear strength of flat slabs. This adjustment takes into consideration the influence of the steel reinforcement ratio in addition to the sizes of the slabs and columns. Here is how the revised equation is put together:

$$V_R = .7\,(f_c')^{0.333}\left(\frac{l_{ch}}{2h}\right)^{0.25}(100\rho)^{0.333} b_{\circ CSA} d \quad (8)$$

Elsanadely et al. [100] formulated an empirical equation to predict the punching shear strength of flat slabs, incorporating the effects of slab depth and utilizing experimental data from the literature. The equation also accounts for the use of high-strength concrete, making it applicable to both steel- and FRP-reinforced slabs when adjustments are made for the distinct material properties of FRP. The following formula represents the equation developed by Elsanadely et al. [100]:

$$V_R = 0.127\ (f_c')^{0.333}\sqrt[0.333]{\rho f_y}\left(1+\frac{8d}{b_{\circ ACI}}\right)\sqrt{1+\frac{125}{d}}\ b_{\circ ACI}d \quad (9)$$

El-Ghandour et al. [22] proposed an adjustment factor $(Ef/Es)^{0.333}$ to the equation in the ACI 318-95 code for estimating the punching shear strength of FRP-reinforced concrete flat slabs. The resulting equation is as follows:

$$V_R = 0.333\ (E_f/E_s)^{0.333}\sqrt{f_c'}\,b_{\circ ACI}d \quad (10)$$

Matthys and Taerwe [14] proposed a modification to the BS 8110 [89] equation for calculating the punching shear strength of FRP-reinforced concrete flat slabs, resulting in the following expression:

$$V_R = 1.36\ (1/d)^{\frac{1}{4}}\left(\frac{100\rho f_c' E_f}{E_s}\right)^{\frac{1}{3}} b_{\circ BS}d \quad (11)$$

Ospina et al. [15] proposed a further adjustment to the equation introduced by Matthys and Taerwe [14], which is formulated as follows:

$$V_R = 2.77\ (\rho_f f_c')^{\frac{1}{3}}(E_f/E_s)^{0.5} b_{\circ BS}d \quad (12)$$

El-Gamal et al.'s proposal [29] included a new factor α to the ACI 318-05 punching shear equation, which can be utilized to approximate the punching shear strength of flat slabs constructed with reinforced concrete and steel. The following is the expression for the altered equation:

$$V_R = 0.333\ \sqrt{f_c'}\ b_{\circ ACI}da \quad (13)$$

$$a = 0.5\ \sqrt[3]{\rho E}\ \left(1+\frac{8d}{b_{\circ ACI}}\right) \quad (14)$$

Bompa and Onet [101] empirically determined the inclination angle of the punching shear surface through a combination of computational calculations and practical experiments gleaned from existing literature. The resulting formula for the inclination angle (θ) is contingent on factors such as the effective depth of the slab, the ratio of flexural reinforcement in the slab, and the yield strength of the reinforcement relative to the compressive strength of the concrete. The following is how this model is stated:

$$\tan\theta = 0.6 + \ \rho f_y/f_c\sqrt{d/265} \quad (15)$$

Moreover, Bompa and Onet [101] devised a punching shear model that incorporates the degree of inclination of the fracture surface, departing from the conventional approach of employing a fixed critical shear perimeter. Here is the formulation of this model:

$$V_R = 2\pi d\ (f_c)^{\frac{1}{3}}[0.4d + \rho f_y^{\frac{1}{3}} r_\circ]\xi \quad (16)$$

where r_o represents the punching shear radius at the top surface of the slab.

$$r_\circ = dcot\theta + c/2$$

$$\xi = 0.75 + (d/lch)^{-0.2}$$

In order to examine the punching shear behavior of two-way flat slabs, Broms [102] developed the Tangential Strain Theory (TST), which incorporates a strut-and-tie failure mechanism near the junction of the column and the slab. This approach emphasizes the importance of considering the yielding of slab reinforcement at the column edge. For slabs with reinforcement remaining within the elastic range, the punching shear strength is determined using the following equation. While originally developed for steel-reinforced slabs, the theory can be adapted for FRP-reinforced slabs by accounting for the distinct stress-strain behavior of FRP materials:

$$V_R = m_\varepsilon \frac{8\pi}{1-\ln(\frac{A}{B})-\frac{A^2}{B^2}} \quad (17)$$

As an alternative, the punching shear may be written as follows if the slab reinforcements are totally yielded:

$$V_{y2} = m_y \frac{2\pi}{1-\frac{A}{B}} \quad (18)$$

In this case, B=3π/8c, where c is the square column's side length and A is the circular test model's diameter.

$$m_\varepsilon = \rho d^2 E_s \varepsilon_s (1 - x/3d)$$

$$m_y = \rho d^2 f_y (1 - x/3d)$$

The depth of the compression zone is shown here by x.

Hassan et al. [35] introduced a punching shear formula for flat slabs reinforced with FRP by combining three suggested variables into the ACI 318-19 [87] framework: βs, βa (similar to JSCE 1997), and βc. Experiments were used to validate these parameters. This is the expression for the equation that Hassan et al. [35] proposed:

$$V_R = \beta_d \beta_p \beta_c \sqrt{f_c'}\, b_{\circ ACI} d \quad (19)$$

where:

$$\beta_d = (\frac{130}{d})^{1/4}$$

$$\beta_p = 0.55(\frac{100\rho_f E_f}{E_s})^{1/3}$$

$$\beta_c = (0.65 + \frac{4d}{b_{\circ ACI}})$$

Drawing on critical shear crack theory, Muttoni et al. [93] presented punching shear design formulations. As a minimum value derived from the above equations, the punching shear strength is offered.

$$V_R = k_b \sqrt[3]{(100\rho f_c \frac{d_{dg}}{r_s})}\, b_o d \tag{20}$$

$$V_R = 0.55 b_o d \sqrt[2]{f_c} \tag{21}$$

Here,

$$k_b = \sqrt{8a\frac{d}{b_o}} \geq 1$$

$$d_{dg} = d_{g0} + d_g.\min\left(\left(\frac{60}{f_c}\right)^2, 1\right) \leq 40mm \tag{22}$$

Here, a represents a factor fixed at 8 for interior columns. d_{dg} indicates the reference crack roughness, whereas d_{g0} and "dg" stand for the reference aggregate size, set at 16 mm, and the maximum aggregate size, respectively..

In the case of concrete slabs and footings reinforced with steel, Kueres et al. [27] revised the punching shear equations in Eurocode 2. Data testing from the literature was used to inform their revision. They promoted the unification of the two distinct equations for calculating punching shear in slabs and footings as required by Eurocode 2. The following is the suggested updated equation:

$$V_R = 2.22\, k_d k_\lambda \sqrt[3]{(100\rho f_{ck})}\, b_{o\,revised}\; d \tag{23}$$

Here, k_d (where k_d=1/(1+d/200)$^{0.5}$) represents the modified influence factor, while k_λ=(b_o/d.a_λ/d)$^{0.5}$, with a_λ representing the shear span.

An empirical equation obtained from substantial experimental data on FRP-reinforced concrete slabs was introduced by Hassan et al. [11]. Here is how this equation is expressed:

$$V_R = \left(\frac{4d}{b_{\circ CSA}} + 0.65\right) 0.065\lambda\left(E_f \rho_f f_c'\right)^{1/3} \left(\frac{125}{d}\right)^{1/6} b_{\circ CSA} d \tag{24}$$

Table 3 - A comparative analysis between the punching shear strength estimates derived from the proposed formula and the measured values found in the literature for FRP-reinforced slabs without shear reinforcement

Reference	$d_{(slab)}$ (mm)	$b_{(column)}$ (mm)	f_c' (MPa)	ρ (%)	E_f(GPa)	V_{Exp} (KN)	$V_{test}/V_{pred.}$
Matthys and Taerwe [14]	95 -126	80-150	32.1-36.3	0.52-3.78	40.7-95	171-347	1.032- 1.562
Hassan et al. [25]	131-281	300-375	29.6-75.8	0.73-1.61	48.1-64.9	386-1600	1.116-1.355
Hassan et al. [19]	132-281	300	34.3-75.8	0.71-1.61	48.2-64.9	329-1600	1.110-1.301
Lee et al. [16]	110	225	36.3	1.1-1.26	48.2	222-248	0.973-1.063
Zhang et al. [103]	100	250	35-71	1.05-1.18	42	218-275	1.10-1.47
Zaghloul and Razaqpur [104]	75	250	44.8	1.33	100	234	1.150
Hussien et al. [105]	100	250	26-40	0.95-1.18	42	210-249	1.205-1.262
Ospina et al. [15]	120	250	28.9-37.5	0.73-1.46	28.4-34	206-260	1.00-1.14
Ahmad et al. [106]	61	75-100	36.6-44.6	0.95	113	78-99	0.893-1.101
Nguyen-Minh and Rovnak [33]	129	200	39	0.48-0.92	48	180-244	0.867-0.946
Gouda and Elsalakawy [107]	159	300	38	0.65	68	421	1.05
Al Ajami [108]	94-191	200	35-53	0.93-1.01	52.5	168-617	0.88-1.17
Gouda and Elsalakawy [26]	160	300	38.0-70.0	0.65-1.13	68	363-425	0.77-0.87
Dulude et al. [18]	131-281	300-450	29.6-44.9	0.71-1.56	48.1-48.2	329-1248	1.08-1.39
Ramzy et al. [109]	82-112	200	33-39.7	0.81-1.54	46	165-230	0.90-1.43

4.2. Predicting Punching Shear Capacity of Punching Shear Strength of FRP-RC Slab-Column Connections without Shear Reinforcement Using Machine Learning Model

Machine learning (ML) stands as a pivotal artificial intelligence tool, adept at autonomously absorbing and refining its operations through pre-existing data [110]. In contrast to conventional regression analysis, ML boasts heightened predictive precision and adeptness in managing intricate datasets [112]. It finds extensive application across various domains, ranging from assessing concrete material properties to evaluating the load-bearing capacity of reinforced concrete elements [113–120]. Classical machine learning frameworks include

backpropagation artificial neural networks (BPANN), support vector regression (SVR), decision trees, random forests (RF), and gradient boosting regression trees (GBRT) [113, 115-119]. Although frequently used, the study of machine learning for estimating the punching shear capacity of FRP bar-reinforced concrete flat slabs is still in its early stages. Metwally [121] used an artificial neural network (ANN) to predict punching shear capacity from a dataset of 59 flat slabs, whereas Vu and Hoang [122] used the support vector machine approach in a similar attempt. Liang's recent contributions [123, 124] have increased the dataset to 154 items, using sophisticated ensemble prediction machine learning techniques and evolutionary algorithms to generate explicit expressions. These developments have significantly improved prediction accuracy and resolved application restrictions, demonstrating the superiority of machine learning models in estimating punching shear capacity over previous empirical techniques.

Yan et al. [125] performed a thorough analysis and created a complete database with 165 sets of test data, including eight critical variables required for model creation. They then developed four data-driven models—backpropagation artificial neural network (BPANN), support vector regression (SVR), random forest (RF), and gradient boosting regression tree (GBRT)-and compared their performance to conventional prediction algorithms. To improve model interpretability, the study used the Shapley Additive Explanation (SHAP) and Partial Dependence Plot (PDP) techniques to quantify the influence of parameters on anticipated outcomes. The results showed that Ju et al.'s technique beat the 25 other formulae tested, with R2, Pre/Exp, MAPE, and RMSE values of 0.76, 1.02, 22.2%, and 142.8 kN, respectively. Furthermore, machine learning methods outperformed classical formulae in prediction accuracy, with the GBRT model achieving the best precision. SHAP analysis indicated effective slab height and column section aspect ratio as important variables impacting punching shear capacity, whereas PDP analysis gave quantitative information on how punching shear capacity fluctuates with each relevant variable.

Doğan & Arslan [126] conducted a literature review and gathered experimental data from 141 slabs reinforced with GFRP bars, CFRP bars, and conventional steel bars that had undergone punching. Following data collection, meticulous parameter calibration enabled the development of prediction models for slab punching strength using five different machine learning techniques: Multiple Linear Regression (MLR), Bagging-Decision Tree Regression (Bagging-DT), Random Forest Regression (RF), Support Vector Regression (SVR), and Extreme Gradient Boosting (XGBoost). The study thoroughly examined the convergence performance of the algorithms concerning the outcomes, alongside analyzing the impact of each parameter on the data. It also critically evaluated the predicted accuracy for punching strength in the literature, including ACI 440's and other techniques. The study's most notable conclusion was that predictions, especially those derived from building codes, tended to be more conservative than experimental results. Among the methods employed, Support Vector Regression (SVR) emerged as the most efficient, particularly in estimating the strength of slabs reinforced with GFRP bars. Following analysis, SVR yielded impressive results: for slabs reinforced with GFRP bars, the R2 values, Mean Absolute Error (MAE), and Root Mean Squared Error (RMSE) performance measures significantly exceeded those of empirical correlations, reaching 96.23%, 0.16, and 0.19, respectively.

Here's the revised version of the paragraph, taking into account the note that ACI is "safe for design purposes" and should not be labeled as "least reliable". The author of this article has also clarified other aspects and ensured consistency:

In their investigation of the punching shear strength of fiber-reinforced polymer (FRP) concrete slabs, Badra et al. [127] assessed several models from the literature using a rudimentary reliability analysis, highlighting the need for more precise and consistent strength models. As a result, the study proposed two machine learning (ML) models, both of which demonstrated superior accuracy in predicting strength compared to earlier models, offering a novel approach. The study also examined the complex interplay of factors influencing punching shear strength, contrasting the impact of primary variables on strength using the proposed models with that of existing models. A more comprehensive analysis was suggested, with a streamlined reliability-based assessment that ranked CSA as the most dependable. While ACI was not the least reliable, it was considered more conservative and showed less alignment with test data trends. However, it remains a reliable approach for design purposes due to its safety focus. The study revealed that the reliability of the models deteriorated for slabs with thicknesses below 200 mm and reinforcement ratios below 1%. Interestingly, the reliability index remained consistent as concrete compressive strength, effective depth, flexural reinforcement ratio, and Young's modulus increased. Additionally, as these parameters increased, sensitivity factors decreased. Parametric experiments using an ANN model and an SVM model demonstrated enhanced accuracy, consistency, and safety. These models were capable of accommodating variable uncertainty and accurately capturing the complex behavior of FRP-reinforced concrete slabs under punching shear. The study concluded that, while the flexural reinforcement ratio had minimal impact on strength due to the reduced transverse resistance of FRP reinforcement, the size and compressive strength of the concrete significantly influenced strength, likely due to the values of Young's modulus of FRP bars and reduced dowel action effects.

In order estimate the punching shear strength of FRP-C slabs without shear reinforcement, Truong et al. [128] used machine learning (ML) approaches. Using input variables like the shear span-to-effective depth ratio, column perimeter-to-effective depth ratio, effective slab depth, concrete compressive strength, FRP reinforcement ratio, ultimate tensile strength, and elastic modulus of FRP, they created an experimental database with 104 specimens. The study evaluated the applicability of three ML techniques: extreme gradient boosting (XGBoost), random forest (RF), and support vector regression (SVR). To refine hyperparameters, ML-based models were developed using a grid search method and a 5-fold cross-validation strategy. Using a variety of statistical estimators, the effectiveness of these machine learning-based models was assessed and contrasted with the design codes and pre-existing models. The results indicated that there was no apparent bias in the predictions of punching shear strength by the three ML-based models concerning the input variables. With a coefficient of determination (R2) of 0.962, a root mean square error (RMSE) of 0.061 MN, a mean absolute error (MAE) of 0.035 MN, and a mean absolute percent error (MAPE) of 8.931% for the testing dataset, the XGBoost-based model emerged as exhibiting the most superior prediction performance. Further analysis revealed that the effective slab depth exerted the most significant impact on prediction performance. When compared to SVR- and RF-based models, as well as existing design codes and models, the XGBoost-based model demonstrated superior accuracy and robustness. These findings underscored the precision and reliability of the XGBoost-based model for FRP-RC slab design and assessment.

5. THE CAPACITY OF FRP-RC SLAB-COLUMN CONNECTIONS TO RESIST PUNCHING SHEAR WHEN INCORPORATING SHEAR REINFORCEMENT

Shear reinforcement can notably enhance punching shear capacity, despite the fact that many slabs are frequently constructed without it due to relatively lenient code requirements and challenges associated with anchoring and installation [87]. Similar to RC slab-column connections with shear reinforcement, punching shear failure in FRP-RC slab-column connections with FRP shear reinforcement may be categorized into three main failure modes depending on the amount and detailing of the FRP shear reinforcement: (1) failure at the level of maximum punching shear capacity, (2) failure outside the shear-reinforced zone, and (3) failure within the shear-reinforced zone [27, 129]. The first mode, shown in Figure 5(a), happens when there is not enough shear reinforcement to stop shear cracks from spreading across the FRP shear reinforcement. This is frequently the result of inadequate shear reinforcement-concrete interaction or anchorages coming loose. Conversely, the second mode, illustrated in Figure 5(b), occurs when there is an excess of shear reinforcement or when the spacing between the shear reinforcement is dense enough. Here, the shear reinforcement halts the propagation of the shear crack, leading to punching shear failure at the maximum punching shear capacity level. This typically transpires at the critical section, positioned between the innermost perimeter of the FRP shear reinforcement and the column edge. In cases where the shear-reinforced zone is relatively short in length, the third mode (depicted in Figure 5(c)) may manifest.

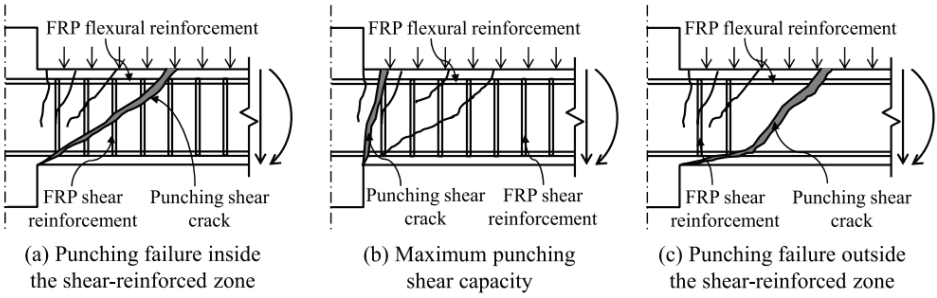

Figure 5 - FRP-RC slab-column connections with FRP shear reinforcement show punching shear failure mechanisms [27].

El-Ghandour et al. [22] investigated eight internal connections between circular slabs and columns, with three incorporating CFRP shear bands as shear reinforcement at varying flexural reinforcement ratios. The introduction of CFRP shear bands enhanced deformability compared to unreinforced slabs, with a significant 13.9% increase in punching capacity observed in slabs featuring 0.38% GFRP flexural reinforcement. The authors suggested a strain limit of 0.0045 for shear reinforcement and advocated for a maximum spacing of 0.5d. Furthermore, they recommended relying on only 50% of concrete resistance, consistent with the provisions of the ACI 318-95 code. Similarly, Hassan et al. [25] investigated 10 full-scale slab-column connections categorized into 200 mm or 350 mm series based on thickness. While the flexural reinforcement of all slabs was GFRP, only seven of them incorporated FRP stirrups for shear reinforcement. FRP stirrups notably enhanced shear capacity by 23%

for series II and reduced failure brittleness by 29% for series I. However, in specimens with low reinforcement ratios, flexural reinforcement primarily governed punching shear capacity, suggesting that FRP stirrups could only offer a modest enhancement.

Gouda and El-Salakawy [26] investigated the utilization of a distinctive type of headed-end GFRP studs as shear reinforcement in internal connections. These studs were meticulously positioned in eight lines encircling the central column, creating five and seven parallel peripheral rows of studs, respectively, with 120 mm and 80 mm (0.75d and 0.50d) spacing between stud rows in Connections R-15-75 and R-15-50. The critical segment was situated 3.90d from the column face, beyond the shear-reinforced zone in both configurations, where the studs extended into the slab. Despite the authors' observations of improved rigidity and load-bearing capability in the shear-reinforced connections, the GFRP studs failed to avert the occurrence of brittle punching shear failure, resulting in both connections collapsing within the shear-reinforced zone. Additionally, there was evidence of damage to the shear stud heads. El-Gendy and El-Salakawy [30] employed a comparable arrangement of GFRP shear reinforcement in GFRP-RC slab-column edge connections in a related study. Their analysis revealed that the joint equipped with seven parallel rows of studs along the periphery (spaced at 0.50d) encountered a failure mode characterized by significant deformations due to bending. Conversely, a connection outfitted with merely five parallel rows of studs along the periphery, with a spacing of 0.75 inches between them, experienced failure due to a combined flexural and punching mode.Table 4 displays the test outcomes for interior slabs constructed with FRP reinforcement, specifically featuring FRP shear reinforcement.

Table 4 - The existing test data for interior slabs reinforced with FRP, particularly focusing on the inclusion of FRP shear reinforcement.

Reference	$d_{(slab)}$ (mm)	$b_{(column)}$ (mm)	f_c' (MPa)	ρ (%) (Flexural rein.)	E_f (GPa) (Flexural rein.)	A_s (mm^2) (Shear rein.)	E_f (GPa) (Shear rein.)	V_{Exp} (KN)	$V_{test}/V_{pred.}$
Hassan et al. [25]	131-284	300	29.5-40.2	0.34-1.61	68	71-129	44.6-130.4	514-2024	0.93-1.12
Gouda and El-Salakawy [26]	160	300	42	0.65	63.1-68	113	60	385-401	0.96-0.97
Zaghloul [24]	100	250	45.7-57.6	0.87-1.48	100	100	100	318-328	1.16
Hussein [130]	160	300	43	0.98-1.93	65	71-127	52-68	527-595	1.01-1.08

5.1. Analytical Models for Predicting the Punching Shear Strength of FRP-Reinforced Concrete Slab-Column Connections with Shear Reinforcement

Present design standards lack precise directives for integrating FRP shear reinforcement in FRP-RC slab-column connections. Additionally, there is a scarcity of analytical models for forecasting the punching shear resistance of FRP-RC slab-column connections devoid of shear reinforcement, as delineated in Table 5.

Hassan et al. [25] introduced an equation aimed at assessing the contribution of FRP stirrups, denoted as, to the punching shear capacity in two-way slabs. This suggested equation, which

is shown below, is a modification of the shear design equation for steel specified in CSA/A23.3-04:

$$v_s = 0.7 \frac{\emptyset_f A_{vs} f_{fs}}{b_o s} \tag{23}$$

Incorporating ϕ_f, the factor representing the resistance of FRP reinforcement, the area of the shear reinforcement's cross-section, and the minimum stress in the shear reinforcement f_{fs}, as delineated in the subsequent two equations:

$$f_{fs} = \frac{\left(0.05 \frac{r_o}{d_b} + 0.5\right) f_{fu}}{1.5} \leq f_{bend}$$

$$f_{fs} = 0.004\, E_{fs}$$

In this scenario, where E_{fs} represents the modulus of elasticity of FRP shear reinforcement, b_r indicates the bend radius, d_b stands for the diameter of the bars, f_{fu} denotes the tensile strength of the unstressed section of the stirrup, and f_{bend} characterizes the ability of the FRP stirrup to resist bending.

Gouda and El-Salakawy [26], as well as El-Gendy and El-Salakawy [30], proposed an equation designed to evaluate the role of FRP stirrups. Their method is based on the similarities between the recommendations for steel-reinforced concrete connections between slabs and columns featuring stud shear reinforcement as detailed in CSA/A23.3-14 and ACI 318-14, respectively.

$$v_s = \frac{\emptyset_f A_{vs} f_{fs}}{b_o s} \tag{24}$$

$$v_s = \frac{A_{vs} f_{fs}}{b_o s} \tag{25}$$

Salama et al. [31] presented an equation tailored to assess the function of FRP stirrups. Their method is informed by the similarities observed in the guidelines for steel-reinforced concrete slab-column connections featuring stud reinforcement against shear, as outlined in CSA S806-12 and ACI 440.1R-15, respectively.

$$v_s = \frac{\emptyset_f A_{vs}\, (0.005\, E_{fs})}{b_o s} \tag{26}$$

$$v_s = \frac{\emptyset_f A_{vs}\, (0.004\, E_{fs})}{b_o s} \tag{27}$$

Truong et al. [131], in their study, formulated a design equation for FRP shear reinforcement based on the design principles specified in ACI 440.1R-15 and the methodology established by El-Gendy and El-Salakawy [30]. This equation is represented as follows:

$$v_s = \frac{0.7\, A_{vs}\, \varepsilon_s\, E_{fs}\, (d - c_u)}{s} \tag{28}$$

In the context of this research article, ε_s denotes the strain effectiveness of FRP shear reinforcement, c_u represents the depth of the neutral axis, and d signifies the effective depth of the slab.

Table 5 - Design approaches for slabs reinforced with FRP and featuring FRP shear reinforcement

Model	Equation
Hassan et al. [25]	$v_s = 0.7\frac{\emptyset_f A_{vs} f_{fs}}{b_o s}$
Gouda and El-Salakawy [26]	$v_s = \frac{\emptyset_f A_{vs} f_{fs}}{b_o s}$
El-Gendy and El-Salakawy [30]	$v_s = \frac{A_{vs} f_{fs}}{b_o s}$
Salama et al. [31]	$v_s = \frac{\emptyset_f A_{vs}\,(0.005\, E_{fs})}{b_o s}$
	$v_s = \frac{\emptyset_f A_{vs}\,(0.004\, E_{fs})}{b_o s}$
Truong et al. [131],	$v_s = \frac{0.7\, A_{vs}\, \varepsilon_s\, E_{fs}\, (d - c_u)}{s}$

6. SUMMARY, CONCLUSIONS AND LIMITATIONS

Interest in reinforcing concrete slabs with Fiber Reinforced Polymer (FRP) bars is increasing, particularly for their advantageous properties in harsh environments where conventional steel reinforcement is prone to corrosion. Understanding the punching shear behavior of flat slabs reinforced with FRP bars is crucial because punching shear is a critical failure mode in flat slab floor systems. A review of approximately one hundred studies, both recent and historical, indicates that FRP reinforcement can effectively replace steel reinforcement, addressing the issue of corrosion. Experimental results suggest that while the basic failure mechanism of slab-column connections reinforced with FRP in concrete (FRP-RC) shares similarities with those reinforced with steel, unique strength prediction models are required due to substantial variations in the elastic modulus and stress-strain characteristics of FRP. Moreover, the punching shear resistance of FRP-RC slab-column connections is enhanced with the incorporation of shear reinforcement. In specimens featuring shear reinforcement, the occurrence of brittle punching shear failure is less frequent, and fractures are more evenly distributed. FRP stirrups effectively distribute the shearing forces across the punched shear zone, providing adequate confinement and resistance to hinder the development of significant shear fractures. This ensures that failure predominantly occurs within or outside the shear-reinforced zone, rather than at a singular point. Despite considerable research on FRP, its

widespread adoption in the construction sector, especially in slab-column connections, remains in its infancy, with limited large-scale implementation:

1. While FRP materials offer excellent resistance to corrosion and other environmental factors, long-term performance data, particularly in real-world conditions, is still limited.
2. Although there is growing research on the use of FRP in concrete reinforcement, there are still no universally accepted design codes or guidelines specifically for FRP-reinforced slab-column connections with shear reinforcement.
3. While FRP bars exhibit favorable properties under normal conditions, their behavior under extreme conditions such as high temperatures, fire, or severe seismic events is not as well-documented as that of steel reinforcement.
4. Most existing studies are based on laboratory-scale tests, which may not fully capture the complexities and constraints of actual construction environments. Scaling up these findings to real-world applications involves uncertainties that need to be addressed.
5. Although the use of FRP can reduce the environmental footprint of reinforced concrete structures, the environmental impact of producing FRP materials themselves, including the energy consumption and emissions associated with their manufacture, needs more comprehensive evaluation.

7. FUTURE RESEARCH DIRECTIONS

Based on the evaluation, the following areas are suggested for further research:

1. The bond between FRP bars and concrete differs from that of steel bars, potentially affecting the overall performance of slab-column connections. Further research is needed to understand and improve this interfacial bond behavior to ensure structural integrity.
2. Conducting tests on FRP-reinforced slab-column connections in flat plates with drop panels or column capitals will provide insights into their structural behavior and potential improvements in punching shear strength.
3. Examining the punching shear strength of FRP pre-stressed slab-column connections will help determine the benefits and limitations of pre-stressing techniques in enhancing structural performance.
4. Studying the behavior and strength of FRP-reinforced slab-column connections under quasi-static dynamic loads is essential to evaluate their seismic response and ensure their reliability in earthquake-prone areas.
5. Conduct experimental and field studies to assess the long-term performance of FRP-RC slab-column connections under various environmental conditions, including exposure to freeze-thaw cycles, chlorides, and UV radiation.
6. Explore the punching shear performance of FRP-RC connections under dynamic and cyclic loading, such as seismic or wind-induced forces, to understand their behavior in regions prone to such events.

7. Study the effect of various FRP stirrup configurations and spacing on punching shear resistance to develop optimized design guidelines for shear reinforcement.

References

[1] N. Özyurt, T. A. Söylev, T. Özturan, A. O. Pehlivan, and A. Niş, "Corrosion and Chloride Diffusivity of Reinforced Concrete Cracked under Sustained Flexure", Teknik Dergi, vol. 31, no. 6, pp. 10315–10337, 2020, doi: 10.18400/tekderg.430536.

[2] M. Benredouane, N. Bourahla, A. Ghodbane, and H. Khalfaoui, "Corrosion Rate-Based Adjustment of Plastic Hinge Parameters of Corroded RC Elements", TJCE, vol. 35, no. 2, pp. 103–123, 2024, doi: 10.18400/tjce.1214088.

[3] A.A. Almusallam, "Effect of degree of corrosion on the properties of reinforcing steel bars," Construct. Build. Mater., vol. 15, pp. 361–368, 2001.

[4] H. Yiğiter, A. Beglarıgale, S. Aydın, and B. Baradan, "Corrosion Behavior of Rebars Embedded in Alkali-Activated and Conventional Reactive Powder Concretes", Teknik Dergi, vol. 31, no. 6, pp. 10359–10378, 2020, doi: 10.18400/tekderg.478154.

[5] Goksu, C., Inci, P., & Ilki, A., "Effect of corrosion on bond mechanism between extremely low-strength concrete and plain reinforcing bars," *J. Perform. Constr. Facil.*, vol. 30, no. 3, 04015055, 2016.

[6] R. Patel, "Prevention of corrosion of steel reinforcement in concrete," in: AIP Conference Proceedings, vol. 2158, 2019, pp. 020035-1~7, https://doi.org/10.1063/1.5127159.

[7] A. Zaki, M.A.M. Johari, W.M.A.W. Hussin, Y. Jusman, "Experimental assessment of rebar corrosion in concrete slab using ground penetrating radar (GPR)," Intern.J. Corrosion, vol. 2018, 5389829, 10 pages, https://doi.org/10.1155/2018/5389829.

[8] M. Zaki, A. Tobaa, A. Shehata, F. Mohamed, R. Khalef, Y. Hagras, R. Abou-Ali, M. Farag, A. Ghaly, M. Madi, E.S. Ahmed, Y. El-Maghraby, M. Abou-Zeid, "Potential advantages of basalt FRP bars compared to carbon FRP bars & conventional steel," Aust. J. Civ. Eng., vol. 19, no. 1, pp. 107–122, 2021.

[9] Seyhan, E. C., Goksu, C., Saribas, I., & Ilki, A., "Hybrid use of externally embedded FRP reinforcement for seismic retrofitting of substandard RC columns," *J. Compos. Constr.*, vol. 27, no. 3, 04023022, 2023.

[10] M. A. Çankaya and Ç. Akan, "An Experimental and Numerical Investigation on the Bending Behavior of Fiber Reinforced Concrete Beams", TJCE, vol. 34, no. 1, pp. 59–78, 2023, doi: 10.18400/tjce.1209152.

[11] M. Hassan, E.A. Ahmed, B. Benmokrane, "Punching shear strength of glass fiber-reinforced polymer reinforced concrete flat slabs," Can. J. Civ. Eng., vol. 40, pp. 951–960, 2013.

[12] T.H.-K. Kang, J.W. Wallace, "Punching of reinforced and post-tensioned concrete slab-column connections," ACI Struct. J., vol. 103, no. 4, pp. 531–540, 2006.

[13] J.-W. Kim, C.-H. Lee, T.H.-K. Kang, "Shearhead reinforcement for concrete slab to concrete-filled tube column connections," ACI Struct. J., vol. 111, no. 3, pp. 629–638, 2014.

[14] S. Matthys, L. Taerwe, "Concrete slabs reinforced with FRP grids. II. Punching resistance," J. Compos. Construct., vol. 4, no. 3, pp. 154–161, 2000.

[15] C.E. Ospina, S.D.B. Alexander, J.J. Roger Cheng, "Punching of two-way concrete slabs with fiber-reinforced polymer reinforcing bars or grids," ACI Struct. J., vol. 100, no. 5, pp. 589–598, 2003.

[16] J.H. Lee, Y.S. Yoon, W.D. Cook, D. Mitchell, "Improving punching shear behavior of glass fiber-reinforced polymer reinforced slabs," ACI Struct. J., vol. 106, no. 4, pp. 427–434, 2009.

[17] J.H. Lee, J.M. Yang, Y.S. Yoon, "Rational prediction of punching shear strength of slabs reinforced with steel or FRP bars," Mag. Concr. Res., vol. 62, no. 11, pp. 821–830, 2010.

[18] C. Dulude, M. Hassan, E.A. Ahmed, B. Benmokrane, "Punching shear behavior of flat slabs reinforced with glass fiber reinforced polymer bars," ACI Struct. J., vol. 110, no. 5, pp. 723–734, 2013.

[19] M. Hassan, E.A. Ahmed, B. Benmokrane, "Punching-shear strength of normal and high-strength two-way concrete slabs reinforced with GFRP bars," J. Compos. Construct., vol. 17, pp. 04013003-1~12, 2013.

[20] T.H.-K. Kang, J.W. Wallace, "Seismic performance of reinforced concrete slab-column connections with this plate stirrups," ACI Struct. J., vol. 105, no. 5, pp. 617–625, 2008.

[21] T.H.-K. Kang, J.D. Lee, B.-S. Lee, M.-J. Kim, K.-H. Kim, "Punching and lateral cyclic behavior of slab-column connections with shearbands," ACI Struct. J., vol. 114, no. 5, pp. 1075–1087, 2017.

[22] A.W. El-Ghandour, K. Pilakoutas, P. Waldron, "Punching shear behavior of fiber reinforced polymers reinforced concrete flat slabs: experimental study," J. Compos. Construct., vol. 7, no. 3, pp. 258–265, 2003.

[23] R. Li, Y.S. Cho, S. Zhang, "Punching shear behavior of concrete flat plate slab reinforced with carbon fiber reinforced polymer rods," Composites Part B, vol. 38, no. 5–6, pp. 712–719, 2007.

[24] A. Zaghloul, "Behaviour and Strength of CFRP Reinforced Flat Plate Interior Column Connections Subjected to Shear and Unbalanced Moments," Master Thesis, Department of Civil and Environmental Engineering, Carleton Univ., Ottawa, Canada, 2002.

[25] M. Hassan, E.A. Ahmed, B. Benmokrane, "Punching shear behavior of two-way concrete slabs reinforced with FRP shear reinforcement," J. Compos. Construct., vol. 19, no. 1, pp. 04014030-1~13, 2015.

[26] A. Gouda, E. El-Salakawy, "Behavior of GFRP-RC interior slab-column connections with shear studs and high-moment transfer," J. Compos. Construct., vol. 20, no. 4, pp. 04016005-1~12, 2016.

[27] D. Kueres, P. Schmidt, J. Hegger, "Two-parameter kinematic theory for punching shear in reinforced concrete slabs with shear reinforcement," Eng. Struct., vol. 181, pp. 216–232, 2019.

[28] J.-M. Yang, K.H. Min, Y.-S. Yoon, "Effect of anchorage and strength of stirrups on shear behavior of high-strength concrete beams," Struct. Eng. Mech., vol. 41, no. 3, pp. 407–420, 2012.

[29] S. El-Gamal, E. El-Salakawy, B. Benmokrane, "Behavior of concrete bridge deck slabs reinforced with fiber-reinforced polymer bars under concentrated loads," ACI Struct. J., vol. 102, no. 5, pp. 727–735, 2005.

[30] M. El-Gendy, E. El-Salakawy, "Effect of shear studs and high moments on punching behavior of GFRP-RC slab–column edge connections," J. Compos. Construct., vol. 20, no. 4, pp. 04016007, 2016.

[31] A. Salama, M. Hassan, B. Benmokrane, "Effectiveness of glass fiber-reinforced polymer stirrups as shear reinforcement in glass fiber-reinforced polymer reinforced concrete edge slab–column connections," ACI Struct. J., vol. 116, no. 5, pp. 97–112, 2019.

[32] D.D. Theodorakopoulos, R.N. Swamy, "Analytical model to predict punching shear strength of FRP-reinforced concrete flat slabs," ACI Struct. J., vol. 104, no. 3, pp. 257–266, 2007.

[33] L. Nguyen-Minh, M. Rovnak, "Punching shear resistance of interior GFRP reinforced slab-column connections," J. Compos. Construct., vol. 17, no. 1, pp. 2–13, 2013.

[34] Canadian Standard Association (CSA), "Design and Construction of Building Structures with Fibre-Reinforced Polymer, CSA/S806-12), Canada, Toronto, 2017.

[35] M. Hassan, E.A. Ahmed, B. Benmokrane, "Punching-shear design equation for two-way concrete slabs reinforced with FRP bars and stirrups," Construct. Build.Mater., vol. 66, pp. 522–532, 2014.

[36] Garden HN, Hollaway LC. "An experimental study of the influence of plate end anchorage of carbon fibre composite plates used to strengthen reinforced concrete beams," Compos Struct, vol. 42, no. 2, pp. 175–188, 1998.

[37] Hollaway LC. "A review of the present and future utilisation of FRP composites in the civil infrastructure with reference to their important in-service properties," Constr Build Mater, vol. 24, no. 12, pp. 2419–245, 2010.

[38] Gdoutos EE, Pilakoutas K, Rodopoulos CA. "Failure analysis of industrial composite materials." New York: McGraw-Hill Professional Engineering; 2000. p. 51–108.

[39] Taerwe Luc. "Non-metallic (FRP) reinforcement for concrete structures." Proceedings of the Second International RILEM Symposium vol. 29. CRC Press; 1995.

[40] ACI 440 1R-15. "Guide for the design and construction of structural concrete reinforced with FRP bars." Farmington Hills, MI: American Concrete Institute (ACI); 2007.

[41] ACI 440 Part 6–8. Specification for carbon and glass fiber-reinforced polymer bar materials for concrete reinforcement. Farmington Hills, MI: American Concrete Institute (ACI); 2008.

[42] Al-Sunna Raed, Pilakoutas Kypros, Hajirasouliha Iman, Guadagnini Maurizio.Deflection behaviour of FRP reinforced concrete beams and slabs: an experimental investigation. Compos Part B Eng 2012;43(5):2125–34.

[43] Teng JG, Chen Jian-Fei, Smith Scott T, Lam L. FRP: strengthened RC structures.Front Phys 2002:266.

[44] Burgoyne C. FRP reinforcement in RC structures. Switzerland: International Federation for Structural Concrete (FIB); 2007.

[45] Canadian Standards Association. Specification for fibre-reinforced polymers, (CAN/CSA S807-10). Mississauga, Ont, Rexdale, ON, Canada: Canadian Standards Association; 2010. p. 27.

[46] Bakis CE, Bank LC, Brown V, Cosenza E, Davalos JF, Lesko JJ, et al. Fiber-reinforced polymer composites for construction—state-of-the-art review. J Compos Constr 2002;6(2):73–87.

[47] Aashto L. Bridge design guide specifications for GFRP—reinforced concrete bridge decks and traffic railings. Washington (DC): American Association of State Highway and Transportation Officials; 2009.

[48] Calvi GM, Pavese A, Rasulo A, Bolognini D. Experimental and numerical studies on the seismic response of RC hollow bridge piers. Bull Earthq Eng 2005;3(3):267–97.

[49] Cheng C-T, Mo Y, Yeh Y-K. Evaluation of as-built, retrofitted, and repaired shearcritical hollow bridge columns under earthquake-type loading. J Bridg Eng 2005;10(5):520–9.

[50] Dawood M. Bond characteristic sand environmental durability of CFRP materials for strengthening steel bridges and structures Ph.D thesis Raleigh, NC: North Carolina State Univ.; 2008.

[51] Delgado Pedro, Rocha Patrício, Pedrosa João, Arêde António, Pouca Nelson Vila,Santos Miguel, et al. Retrofitting of bridge hollow piers with CFRP. Proceedings of ECCOMAS Thematic Conference Quot; Computational Methods in StructuralDynamics and Earthquake Engineering 2007.

[52] Dong ZH, Han Q, Du XL, Zhang DJ. Experimental study on seismic performance of CFRP confined RC rectangular hollow section bridge piers. International efforts in lifeline earthquake engineering. 2014. p. 457–64.

[53] Han Qiang, Wen Jianian, Du Xiuli, Jia Junfeng. Experimental and numerical studies on seismic behavior of hollow bridge columns retrofitted with carbon fiber reinforced polymer. J Reinf Plast Compos 2014;33(24):2214–27.

[54] Matta F. Bond between steel and CFRP laminates for rehabilitation of metallic bridges Master's thesis Padua, Italy: Faculty of Engineering, Univ. of Padua; 2003.

[55] Miller Trent C, Chajes Michael J, Mertz Dennis R, Hastings Jason N. Strengthening of a steel bridge girder using CFRP plates. J Bridg Eng 2001;6(6):514–22.

[56] Breña Sergio F, Bramblett Regan M, Benouaich Michaël A, Wood Sharon L, Kreger Michael E. Use of carbon fiber reinforced polymer composites to increase the flexural capacity of reinforced concrete beams. The University Of Texas at Austin; 2001. Research Report no. 1776-1.

[57] Ning Huiming, Li Yuan, Hu Ning, Arai Masahiro, Takizawa Naoya, Liu Yaolu, et al. Experimental and numerical study on the improvement of interlaminar mechanical properties of Al/CFRP laminates. J Mater Process Technol 2015;216:79–88.

[58] Ammar MA. Bond durability of basalt fibre-reinforced polymers (BFRP) bars under freeze-and-thaw conditions Ph.D thesis Dept. of Civil Engineering, Université Laval; 2014. p. 125.

[59] Banibayat P, Patnaik A. Creep rupture performance of basalt fiber-reinforced polymer bars. J Aerosp Eng 2013;28(3):04014074.

[60] Brothers H. Glass fiber reinforced polymer (GFRP) rebar Aslan 100. Seward, Neb. 2001.

[61] Davies Peter, Reaud Yvan, Dussud Loic, Woerther Patrice. Mechanical behavior of HMPE and aramid fibre ropes for deep sea handling operations. Ocean Eng 2011;38(17):2208–14.

[62] Sahu NP, et al. Study on aramid fibre and comparison with other composite materials. Int J 2014;1:303–6.

[63] Palmieri A, Matthys S, Taerwe L. Experimental investigation on fire endurance of insulated concrete beams strengthened with near surface mounted FRP bar reinforcement. Compos Part B Eng 2012;43(3):885–95.

[64] Zhou Jikai, Bi Fengtong, Wang Zhiqiang, Zhang Jian. Experimental investigation of size effect on mechanical properties of carbon fiber reinforced polymer (CFRP) confined concrete circular specimens. Constr Build Mater 2016;127:643–52.

[65] Liu H, Zhao X, Al-Mahaidi R. Effect of fatigue loading on bond strength between CFRP sheets and steel plates. Int J Struct Stab Dyn 2010;10(01):1–20.

[66] Abdelrahman K, El-Hacha R. Cost and ductility effectiveness of concrete columns strengthened with CFRP and SFRP sheets. Polymer 2014;6(5):1381–402.

[67] Das S. The cost of automotive polymer composites: a review and assessment of DOE's lightweight materials composites research. Springfield, VA: American Department of Energy; 2001. p. 1–47.

[68] Delgado Pedro, Arêde António, Vila Pouca Nelson, Rocha Patrício, Costa Aníbal, Delgado Raimundo. R

[69] J. Custo´dio, J. Broughton, H. Cruz, A review of factors influencing the durability of structural bonded timber joints, Int. J. Adhes. Adhes. 29 (2009) 173–185.

[70] R.M. Guedes, J.L. Morais, A.T. Marques, A.H. Cardon, Prediction of long-term behavior of composite materials, Comput. Struct. 76 (2000) 183–194.

[71] R.M. Guedes, Lifetime prediction of polymers and polymer matrix composite structures: failure criteria and accelerated characterization, in: Creep and Fatigue in Polymer Matrix Composites, Elsevier, 2019.

[72] A. Movaghghar, G.I. Lvov, An energy model for fatigue life prediction of composite materials using continuum damage mechanics, Appl. Mech. Mater. 110–116 (2011) 1353–1360

[73] A. Al-Saoudi, R. Kalfat, R. Al-Mahaidi, Investigation into the fatigue life of FRP strengthened concrete structures, Mater. Struct. 55 (6) (2022), https://doi.org/10.1617/s11527-021-01839-y.

[74] Shaaban, A.M., and Gesund, H., "Punching Shear Strength of Steel Fiber Reinforced Concrete Flat Plates," Structural Journal, vol. 91, no. 4, pp. 406-414, Jul. 1994.

[75] E. H. Rochdi, D. Bigaud, E. Ferrier, and P. Hamelin, "Ultimate behavior of CFRP strengthened RC flat slabs under a centrally applied load," Composite Structures, vol. 72, no. 1, pp. 69-78, 2006.

[76] A. Torabian, B. Isufi, D. Mostofinejad, and A. P. Ramos, "Behavior of thin lightly reinforced flat slabs under concentric loading," Engineering Structures, vol. 196, p. 109327, 2019.

[77] ASCE-ACI Committee 426, "The shear strength of reinforced concrete members - slabs," *J. Struct. Div.,* vol. 100, no. 8, pp. 1543–1590, 1974.

[78] American Concrete Institute, "Guide to seismic design of punching shear reinforcement in flat plates," ACI 421.2R, Farmington Hills, MI, ACI, 2010.

[79] R. Lenschow and M. Sozen, "A yield criterion for reinforced concrete slabs," ACI J. Proc., vol. 64, no. 5, pp. 266–273, 1967.

[80] M.D. Kotsovos and M.N. Pavlovic, "Ultimate Limit-State Design of Concrete Structures: A New Approach," Thomas Telford, London, 1998, p. 208.

[81] H.-G. Park, K.-K. Choi, and L. Chung, "Strain-based strength model for direct punching shear of interior slab-column connections," Eng. Struct., vol. 33, pp. 1062–1073, 2011.

[82] P.D. Zararis and G.C. Papadakis, "Diagonal shear failure and size effect in RC beams without web reinforcement," J. Struct. Eng., vol. 127, no. 7, pp. 733–742, 2001.

[83] Banthia, N., Al-Asaly, M., & Ma, S. "Behavior of concrete slabs reinforced with fiber-reinforced plastic grid." Journal of Materials in Civil Engineering, vol. 7, no. 4, pp. 252-257, 1995.

[84] Li, R., Cho, Y. S., & Zhang, S. "Punching shear behavior of concrete flat plate slab reinforced with carbon fiber reinforced polymer rods." Composites Part B: Engineering, vol. 38, no. 5-6, pp. 712-719, 2007.

[85] Hassan, M., Ahmed, E., & Benmokrane, B. "Punching-shear strength of normal and high-strength two-way concrete slabs reinforced with GFRP bars." Journal of Composites for Construction, vol. 17, no. 6, p. 04013003, 2013.

[86] S. K. Shill, E. O. Garcez, R. Al-Ameri, and M. Subhani, "Performance of two-way concrete slabs reinforced with basalt and carbon FRP rebars," Journal of Composites Science, vol. 6, no. 3, p. 74, 2022.

[87] ACI Committee 318-19. Building Code Requirements for Structural Concrete andCommentary. American Concrete Institute; 2019.

[88] CSA-A23.3- 04. Design of concrete structures for buildings. Canadian Standards Association 2004.

[89] British Standards Institution. Structural use of concrete, part 1: code of practice for design and construction. BS 8110-1; 1997.

[90] CEB–FIP. 1990. Model Code: Bulletin D'Information No. 203– 305. Comit´e Euro–International Du B´ eton – F´ed´ eration de la Pr´econtrainte; 1990.

[91] FIB 2001. Punching of structural concrete slabs. Lausanne: InternationalFederation for Structural Concrete; 2001.

[92] Lantsoght E. Literature Review of Punching Shear in Reinforced Concrete Slabs. Research Report No. 09-10; 2009, Georgia Institute of Technology.

[93] Muttoni A, Schwartz, J. Behaviour of Beams and Punching in Slabs without Shear Reinforcement. IABSE Colloquium 1991; 62: 703-08, Zurich, Switzerland.

[94] Japan Society of Civil Engineers (JSCE). Recommendation for design and construction of concrete structures using continuous fibre reinforcing materials. Concrete Engineering, Series 23, A. Machida, ed., 1997.

[95] ACI Committee 440. Guide for the design and construction of concrete reinforced with FRP bars (ACI 440.1R-15). American Concrete Institute; 2015.

[96] CAN/CSA S806-12. Design and construction of building structures with fibre reinforced polymers. Canadian Standards Association; 2012.

[97] Rizk E, Marzouk H, Hussein A. Punching shear of thick plates with and without shear reinforcement. ACI Struct J 2011;108(5):581–91.

[98] Zhou P, Barr B, Lydon F. Fracture properties of high strength concrete with varying silica fume content and aggregates. Cem Conc Res 1995;25(3):543– 52. https://doi.org/10.1016/0008-8846(95)00043-C.

[99] Rizk E, Marzouk H, Hussein A, Hossin M. Effect of reinforcement ratio on punching capacity of RC plates. Can J Civ Eng 2011;38:729–40. https://doi.org/10.1139/L11-053.

[100] Elsanadedy HM, Al-Salloum YA, Alsayed SH. Prediction of punching shear strength of HSC interior slab-column connections. KSCE J Civil Eng 2013;17(2):473–85. https://doi.org/10.1007/s12205-013-1971-8.

[101] Bompa DV, Onet¸ T. Punching shear strength of RC flat slabs at interior connections to columns. Mag Concr Res 2016;68(1):24–42. https://doi.org/10.1680/macr.14.00402

[102] Broms CE. Tangential strain theory for punching failure of flat slabs. ACI Struct J2016;113(1):95–104. https://doi.org/10.14359/51687942.

[103] Zhang Q, Marzouk H, Hussein A. A Preliminary Study of High-Sstrength concrete two-way slabs reinforced with GFRP bars. Proc., 33rd CSCE Annual Conf.: General Conference and International History Symposium, Canadian Society of Civil Engineers; Toronto, ON, Canada; 2005.

[104] Zaghloul A, Razaqpur A. Punching Shear Strength of Concrete Flat Plates Reinforced with CFRP Grids. Proc., 4th Int. Conf. on Advanced Composite Materials in Bridges and Structures, CSCE, Calgary, AB, Canada; 2004

[105] Hussein A, Rashid I, Benmokrane B. Two-Way Concrete Slabs Reinforced with GFRP Bars. Proc., 4th Int. Conf. on Advanced Composite Materials in Bridges and Structures, Canadian Society of Civil Engineers; Calgary, AB, Canada; 2004.

[106] Ahmad SH, Zia P, Yu TJ, Xie Y. Punching shear tests of slabs reinforced with 3-D carbon fiber fabric. Conc Int 1993;16(6):36–41.

[107] Gouda A, El-Salakawy E. Behaviour of GFRP-RC interior slab-column connections with shear studs and high-moment transfer. J Comp Constr (ASCE) 2016;20(4). https://doi.org/10.1061/(ASCE)CC.1943-5614.0000663.10.1061/(ASCE) CC.1943-5614.0000663.

[108] Ajami AL. Punching shear of concrete flat slabs reinforced with fiber reinforced polymer bars. University of Bradford; 2018. PhD thesis

[109] Ramzy ZZ, Salma MT. Punching behavior and strength of two-way concrete slab reinforced with glass-fiber reinforced polymer (GFRP) rebars. Structural Composites for Infrastructures Applications Conference. 2007

[110] Y. Yu, G.H. Fang, R. Kurda, et al., An agile, intelligent and scalable framework for mix design optimization of green concrete incorporating recycled aggregates from precast rejects, Case Stud. Constr. Mat. (2024) e03156.

[111] V. Shobeiri, B. Bennett, T.Y. Xie, et al., Mix design optimization of waste-based aggregate concrete for natural resource utilization and global warming potential, J. Clean. Prod. (2024) 141756.

[112] H. Xue, H. Guan, B.P. Gilbert, X. Lu, Y. Li, Simulation of punching and post-punching shear behaviours of RC slab–column connections, Mag. Concr. Res. 73 (22) (2021) 1135–1150.

[113] Y. Yu, T.Y. Hu, Machine learning based compressive strength prediction model for CFRP-confined columns, KSCE J. Civ. Eng. 28 (1) (2024) 315–327.

[114] T. Liu, Z. Wang, Z. Long, J. Zeng, J. Wang, J. Zhang, Direct shear strength prediction for precast concrete joints using the machine learning method, J. Bdg Eng.27 (5) (2022) 04022026.

[115] Y.X. Shen, L.F. Wu, S.X. Liang, Explainable machine learning-based model for failure mode identification of RC flat slabs without transverse reinforcement, Eng.Fail Anal. 141 (2022) 106647.

[116] L. Lin, J.J. Xu, J.C. Yuan, et al., Compressive strength and elastic modulus of RBAC: an analysis of existing data and an artificial intelligence based prediction, Case Stud. Constr. Mat. 18 (2023) e02184.

[117] S.X. Liang, Y.X. Shen, X.D. Ren, Comparative study of influential factors for punching shear resistance/failure of RC slab-column joints using machine-learning models, Struct 45 (2022) 1333–1349.

[118] D.C. Feng, W.J. Wang, S. Mangalathu, E. Taciroglu, Interpretable XGBoost-SHAP machine-learning model for shear strength prediction of squat RC walls, J. Struct. Eng. 147 (11) (2021) 04021173.

[119] S.X. Liang, Y.Q. Cai, Z.Y. Fei, et al., Multi-objective optimization design of FRP reinforced flat slabs under punching shear by using NGBoost-based surrogate model, Buildings 13 (11) (2023) 2727.

[120] Y. Yu, X.Y. Zhao, J.J. Xu, S.C. Wang, T.Y. Xie, Evaluation of shear capacity of steel fiber reinforced concrete beams without stirrups using artificial intelligence models, Mater 15 (7) (2022) 2407.

[121] I.M. Metwally, Prediction of punching shear capacities of two-way concrete slabs reinforced with FRP bars, HBRC J. 9 (2013) 125–133

[122] D.T. Vu, N.D. Hoang, Punching shear capacity estimation of FRP-reinforced concrete slabs using a hybrid machine learning approach, Struct. Infrastruct. Eng. 12 (9) (2016) 1153–1161.

[123] S.X. Liang, Y.X. Shen, X.L. Gao, et al., Symbolic machine learning improved MCFT model for punching shear resistance of FRP-reinforced concrete slabs, J. Build. Eng. 69 (2023) 106257.

[124] Y.X. Shen, J.H. Sun, S.X. Liang, Interpretable machine learning models for punching shear strength estimation of FRP reinforced concrete slabs, Crystals 12 (2022) 259.

[125] J. Yan, J. Su, J. Xu, K. Hua, L. Lin, and Y. Yu, "Explainable Machine Learning Models for Punching Shear Capacity of FRP Bar Reinforced Concrete Flat Slab without Shear Reinforcement," *Case Studies in Construction Materials*, vol. e03162, 2024.

[126] G. Doğan and M. H. Arslan, "Determination of punching shear capacity of concrete slabs reinforced with FRP bars using machine learning," *Arabian Journal for Science and Engineering*, vol. 47, no. 10, pp. 13111-13137, 2022.

[127] N. Badra, S. A. Haggag, A. Deifalla, and N. M. Salem, "Development of machine learning models for reliable prediction of the punching shear strength of FRP-reinforced concrete slabs without shear reinforcements," *Measurement*, vol. 201, p. 111723, 2022.

[128] Truong, G. T., Hwang, H. J., & Kim, C. S. (2022). Assessment of punching shear strength of FRP-RC slab-column connections using machine learning algorithms. Engineering Structures, 255, 113898.

[129] S. Lips, M. Fernandez ´ Ruiz, A. Muttoni, Experimental investigation on punching strength and deformation capacity of shear-reinforced slabs, ACI Struct. J. 109 (2012) 889–900

[130] A.M.H. Hussein, Punching Shear Behaviour of GFRP-RC Slab-Column Interior Connections with High Strength Concrete and Shear Reinforcement, Master Thesis, University of Manitoba, Canada, 2017.

[131] G. T. Truong, K. K. Choi, and C. S. Kim, "Punching shear strength of interior concrete slab-column connections reinforced with FRP flexural and shear reinforcement," *Journal of Building* Engineering, vol. 46, p. 103692, 2022.